Desalination and Water Treatment
www.deswater.com
doi: 10.5004/dwt.2022.28040

249 (2022) 191–203
February

The impact of ionic strength and pH on the interaction of *Pseudomonas putida* to minerals and electrical potential of surfaces

Fathiah Mohamed Zuki[a,*], Robert G.J. Edyvean[b], Umi Fazara Md Ali[c], Hamed Pourzolfaghar[a], Hasan Fouzi S. Gafri[a], Mahyoub I. Bzour[a]

[a]*Department of Chemical Engineering, University Malaya, 50603 Kuala Lumpur, Malaysia, Tel. +6019 6090504/+603 79676879; Fax: +603 7967 1378; emails: fathiahmz@um.edu.my (F.M. Zuki), h_pourzolfaghar@yahoo.com (H. Pourzolfaghar), hasan.gafri@yahoo.com (H.F.S. Gafri), mahyoubbzour@gmail.com (M.I. Bzour)*
[b]*Chemical and Biological Engineering Department, University of Sheffield, Newcastle Street, Sheffield S1 3JD, UK, Tel. +44 114 2225776; Fax: +44 114 2225701; email: r.edyvean@sheffield.ac.uk*
[c]*Chemical Engineering Programme, Faculty of Chemical Engineering Technology, Universiti Malaysia Perlis, Kompleks Pusat Pengajian Jejawi 3, 02600 Arau, Perlis, Malaysia, Tel. +6019 5747680; Fax: +6049798636; email: umifazara@unimap.edu.my*

Received 12 August 2021; Accepted 4 December 2021

ABSTRACT

The impacts of the acidity and ionic strength of the solutions were evaluated on the electrical potential of the surfaces as well as the interaction of *Pseudomonas putida* to quartz and hematite. Zeta potential analysis was performed using the streaming potential technique. Experimental results were performed by the flow cell method. Finally, the extended Derjaguin–Landau–Verwey–Overbeek (XDLVO) theory has been applied to describe bacterial-mineral attachment in terms of the sum of repulsive acid-base and electrostatic interaction energies, and attractive van der Waals interaction energies. The results indicate that the zeta potential is obviously influenced by the presence of bacteria, electrolyte concentration, and pH regions. At higher ionic strengths, charge effects on the bacterial cell surface increase adherence by suppressing the thickness of the diffuse double layer. At pH 5–6, at all ionic strengths, the bacteria adhered more on the surfaces of the minerals. Hematite coupons represented the greatest adhesion at pH 5–6 and an ionic strength 0.1 M. XDLVO theory for the attachment of *P. putida* to the minerals also confirmed the experimental outcomes. The information obtained in this study is of fundamental significance for the understanding of the survival and transport of bacteria in water distribution, groundwater, and soil systems.

Keywords: Flow-cell technique; Hematite; Initial interaction; Mineral; *Pseudomonas putida*; Quartz; Extended Derjaguin–Landau–Verwey–Overbeek

1. Introduction

Countless man-made procedures have been impacted by the adherence capability of the bacterial which result to the formation of biofilms [1–5]. Formation of biofilms can have beneficial [5–11] or detrimental/hazardous [12–17] consequences. Nevertheless, the structure and development of biofilms heavily rely on the initial stages of bacterial adhesion [18,19]. In water distribution and groundwater systems, they may cause contamination of drinking water with pathogens such as *Legionella* sp. and *Pseudomonas putida*, and biofilm development on stainless steel in mains water systems [20,21]. *P. putida* strains are abundant in soil and water but have also been reported as opportunistic human pathogens capable of causing nosocomial infections [22–24]. Various kinds of minerals have been used for better bacterial adhesion to minerals investigations, such as hematite, quartz, kaolinite, montmorillonite, and goethite,

* Corresponding author.

to name a few [25–27]. Hematite and quartz are the main mineral types that can easily be found in crust [28,29]. Physico-chemical properties of a mineral surface play a critical role in bacterial adhesion. Electro-kinetic potential is the potential difference between the dispersion medium and the stationary layer of fluid attached to a particle that can be measured experimentally through zeta potential analysis [30]. In the interfacial double layer, the electric potential is located at the slipping plane between the Stern layer and the diffusion layer, and these layers form the electrical double layer (EDL). The interaction between mineral grains and fluid generates the electro-kinetic potentials. In the Stern layer, the negatively charged surface of the mineral grain adsorbs positive ions from the fluid in the immediate vicinity of the grain surface. The zeta potential is used to quantify the magnitude of electrical charge at the double layer and it is a measure of the charges carried by particles suspended in an electrolyte solution. Colloids with high and/or low zeta potential are electrically stable. Ionic strength and acidity of the solutions are critical factors affecting on the bacterial/mineral interactions [31].

The focus of this investigation lies in studying how ionic strength and pH of a salt solution and the size of the mineral grains affect zeta (ζ) potential values. In addition, experimental and theoretical (extended Derjaguin–Landau–Verwey–Overbeek) investigations for the bacterial adhesion to the hematite and quartz minerals have been performed to quantify the initial adsorption of *P. putida* to the mineral surfaces.

2. Material and methods

2.1. Bacteria and mineral preparation for zeta potential analysis

Pseudomonas putida sp. strain ATCC 11172 from Kroto Research Institute, UK, was used for this study. The cells were grown in LB broth containing 1% peptone 140, 0.05% yeast extract and 0.5% sodium chloride at temperature 30°C. Cells were harvested at the final stage of growth (after 24 h). Then, the cells were centrifuged for 15 min at 4,000 g using an Eppendorf centrifuge (5804R, Hamburg, Germany). The growth pallet was then washed in 10 mM NaCl solution, suspended using a vortex vibrator, and centrifuged. Centrifugation and rinsing steps were repeated twice with fresh electrolyte solution to ensure the total separation of bacterium. The electrolytes solution used were prepared with ultrapure water (PURELAB Ultra, ELGA) and reagent grade NaCl (Fisher Scientific, SRG UK) with no pH adjustment (~ pH 6) in microbiological safety cabinet.

Mineral hematite (Rock Shop, Huddersfield UK) and quartz (Geo Supplies Ltd., Sheffield UK) were used in this experiment. These minerals were ground and crushed using a percussion mortar and sieved to <10 μm mineral powder, 50–250 μm, and 500–1,000 μm. The grains were then washed using UHQ water, dried in air at room temperature, and stored in separate labelled sample bag.

2.1.1. Zeta potential analysis

The zeta (ζ) potential of the minerals in various grain sizes were determined by the streaming potential method, using a clamping cell connected with an electrokinetic analyzer (EKA) (Anton Paar GmbH, Graz, Austria). Two electrodes were inserted into the ends of the clamping cell and connected to an electrometer. As the streaming solution is forced to pass through the grains, the accumulation of ions around the grains set up the electric field. The potential of this field is the streaming potential detected by the electrodes. The potential readings are automatically stored and displayed for data processing. Initially, 1 g of mineral grains was placed in the clamping cell (1 cm inside diameter and 15 cm length). The cell was flushed and rinsed under 20 mbar with 70% ethanol and ultrapure water several times and finally rinsed with 0.01 NaCl electrolyte only for titration from pH 11 to pH 2 at a constant pressure difference of 500 mbar. The experiments under the same conditions were then run for the bacteria. 10 mL bacterial suspension was placed in 600 mL of 0.01 M NaCl and automatically titrated before the streaming potential was measured. The same procedure was repeated for both mineral types and sizes at three different electrolyte concentrations (0.01 M, 0.05 M, 0.1 M) with and without bacterial suspensions. Table 1 represents the optimal conditions and EKA measurement parameters were selected based on manufacturer recommendation.

2.2. Mineral and bacteria preparation for flow-cell technique

For the flow-cell experiments, hematite and quartz were cut into coupons 1 cm length × 1 cm width × 0.2 cm depth using a diamond saw and ground using 220 μm grit silicon carbide on a steel lap. The minerals were washed with ultra-pure water and sterilized prior to use by sonication in 2% SDS for 45 min followed by sonication in sterile

Table 1
Operational parameters and optimal EKA conditions

Temperature	25°C
Atmosphere	Nitrogen
Sample size	1 g
Grain sizes	10–1,000 μm
Electrolyte solution	0.01 NaCl
Titration	Started from pH of 11 to 2
Titration for decreasing pH	0.1 N HCl
Titration for increasing pH	0.1 N KOH
Cell pressure program	
Max. pressure	500 mbar
Measurement time	30 s
No. of repetitions	1
Cell rinse program	
Max. pressure	20 mbar
Time in bypass	5 s
Time in cell	5 s
No. of repetitions	1
Automated titration program	
pH difference between measurements	1
Initial amount of titrant	0.2 mL

ultra-pure water for 45 min. These coupons were then kept in ultra-pure water ready for the flow-cell experiment.

P. putida stains were cultured from laboratory stock in LB medium at 30°C. The cells were rinsed with 8% NaCl solution. After addition of medium, centrifugation and measuring, a suspension with optical density of 1.0 (about 10^8 cells/mL) was prepared. The bacteria suspension was diluted three times and the number of bacteria in final diluted suspension was measured as 0.1 OD (±50 cells/mL). 1.5 mL of the final bacteria suspension was stained with 1.5 μL SYTO 9 and held in the dark for 30 min. 0.5 mL of the stained suspension was added to 30 mL of 0.01 M NaCl at a pH of 5–6. Similar portions of the stained bacteria suspension were added to the same electrolyte solution at pH 10–11 and pH 2–3.

2.2.1. Flow cell experiment

The experiments were conducted using a 16 cm × 1 cm × 2 mm parallel flow chambers containing a 20 mm^2 flow cell and a recess of 100 mm^3 for the mineral coupons to sit in, allowing flow over the mineral surface (Fig. 1). A hole was cut in the cell above the mineral where a glass coverslip was placed allowing the mineral to be viewed under the microscope. It was clamped in place by 4 screws and butyl-rubber gasket to ensure an airtight seal. The experimental system was designed to evaluate bacterial attachment on the mineral coupons. The small height (2 mm) of the chamber makes sure that the flow is laminar and steady over the mineral surface. The cell chamber was constructed to allow continuous flow of liquid over the target mineral surface.

A bacterial suspension with approximately 1 × 10^8 cells/mL of *P. putida* in the desired NaCl concentration and pH was passed over the mineral coupon for 30 min at flow rate of 1 mL/min under laminar flow (Re = 0.16) using a peristaltic pump. All experiments were carried out at 25°C. The flow chamber was rinsed with a flow of 70% ethanol for 10 min, Milipore ultra-pure water for 10 min, and with 0.01 M NaCl for 10 min before and after each sample experiment.

Before the experiment being conducted, the microscope needs to be adjusted and focused to the mineral surface. This allows attachment of the bacteria to be seen clearly. Fig. 2 shows micrographs of mineral surfaces for both hematite and quartz.

P. putida attachment was imaged in situ using an epi-fluorescence microscope under 40× magnifications every minute for 30 min flowing period. Where attachment was witnessed, *P. putida* was pumped over the mineral coupon for up to 1 h. Changes in cell number per minute were then assessed by calculating the number of bacteria attached on the mineral surface.

To study the influence of pH and ionic strength on attachment rates of *P. putida* to the two mineral surfaces, bacterial solutions of defined pH and ionic strength were flowed over the surfaces through the flow chamber. Experiments were run for solutions with ionic strength of 0.01 M, 0.05 M, and 0.1 M NaCl at pH 2–3, pH 5–6, and pH 10–11, adjusted by the addition of 0.1 M NaOH and 0.1 M HCl solutions. Photographs were taken every 5 for 30 min and plotted against time as an indicator of cell concentration per area (2 μm). The experimental conditions and the other parameters are shown in Table 2:

3. Results and discussion

3.1. Impact of pH, ionic strength, and grain size on the electrical potential of the hematite and quartz surfaces

The role of ionic strength, pH, and grain size in determining the zeta potential of a bacterium-mineral interaction has been surveyed in this section. Fig. 3 presents the zeta potential results of hematite grains (50–250 μm) with and without *P. putida* at different ionic strengths as a function of pH. As it can be depicted from the samples without *P. putida*, the hematite's surface has a positive charge in the acidic region (pH 2–5) and a negative charge in the alkaline region (pH 6–10). The zeta potentials for various ionic concentrations (0.01, 0.05, and 0.1) are closer together in the region of pH 2 to 5 and further apart for pH 6 to 10. The point of zero charge (PZC) occurs at pH 3.5. A high

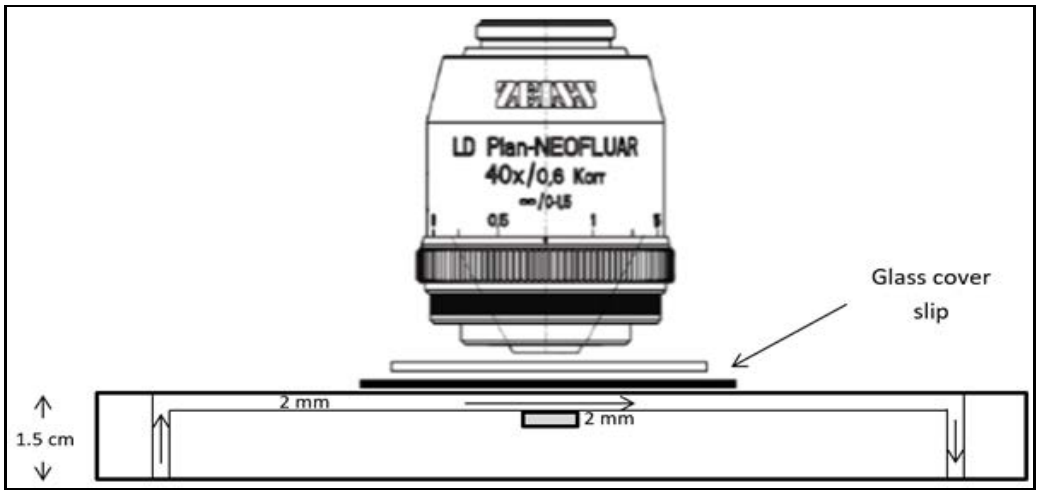

Fig. 1. Schematic diagram for the flow-cell deposition experiment.

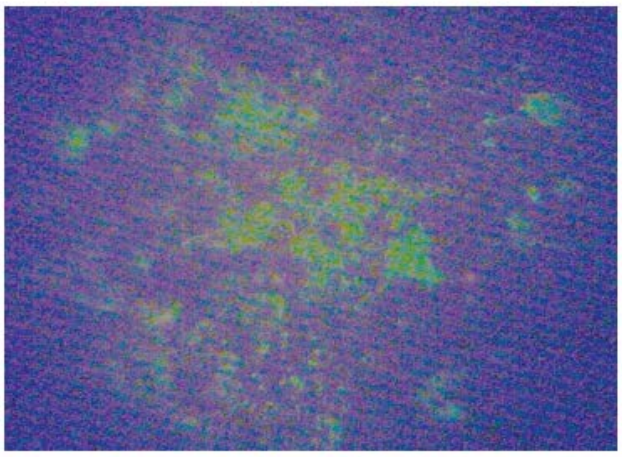

a)

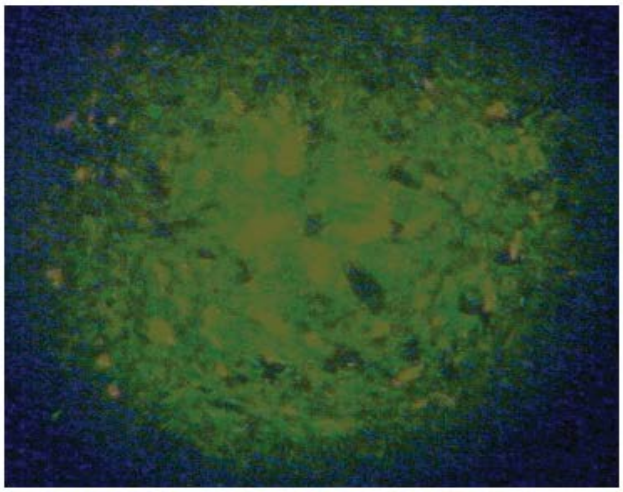

b)

Fig. 2. Actual mineral surface under 40× magnification for (a) hematite and (b) quartz before experiment.

Table 2
Characteristics of the flow generated by a 30 mL fluid at the pump speed of 1 mL/min

Parameter	Value
Dimensions (L.b.2h)	160.10.2 mm^3
Viscosity of fluid	0.01 Pa·s
Density of fluid	1,000 g/mL
Re (Reynolds number)	0.16
Shear rate	9 s^{-1}
Entrance length	0.01 mm

negative potential was obtained for hematite in 0.01 M NaCl solution at pH 6–10 (ζ = –15 mV) followed by 0.1 M and 0.05 M at about ζ = –7 mV.

When the same size hematite grains were interacted with bacteria, the results were different at all pH regions. The high negative charge, observed in Fig. 3, was predictable due to the presence of the negatively charged *P. putida* [32]. Interesting changes in zeta potential were observed at concentrations of 0.01 M and 0.05 M. In the acidic region, between pH 2 to pH 5, the zeta potential values were similar for experimental conditions at 0.01 and 0.05 M, but the values at 0.01 M is significantly lower than the other two ionic strength at pH range from 5 to 11. A direct comparison between hematite only and hematite-*P. putida* (50–250 μm) clearly shows that the values of zeta potentials of hematite-*P. putida* for the three ionic strengths are more negatively charged than those of hematite only. The differences are most marked for 0.1 M at low pH and all solutions at high pH. However, zeta potential values of both hematite conditions (with and without bacteria) are higher at greater ionic strengths (i.e., at pH 10, the zeta potential increased from ζ = –15 mV at 0.01 M to ζ = –5 mV at 0.05 M for hematite only, and from ζ = –45 mV to ζ = –25 mV for hematite-*P. putida* interactions at the comparative ionic strengths).

The zeta potential of larger hematite grains (500 to 1,000 μm) with and without bacteria is shown in Fig. 4. The zeta potential at 0.1 M is more negatively charged compared to other ionic strengths with no bacteria. There is little difference between the zeta potentials of 0.01 and 0.05 M at pH 3 to pH 7, but they do more apart at both very high acidic and alkaline pH. The point of zero charge of hematite changed from pH 4.8 in ionic strength of 0.01 and 0.05 M to about pH 2.9 at 0.1 M electrolyte concentration which is unusual. The PZC of metal oxides is not usually affected by ionic strength and this change might be from impurities with inherent charge. This result is in agreement with previous reports [33].

In the presence of *P. putida*, the 500–1,000 μm hematite grains showed different behaviour to that with no bacteria, especially for ionic strengths of 0.01 M, where the zeta potential has the highest positive charge at the lowest pH and highest negative charge and the highest pH value. Similar trends were obtained for all the tested ionic strengths as with hematite 50–250 μm in the presence of *P. putida* (Fig. 3). Based on the results, zeta potentials are higher at low ionic strength in the alkaline region. In 0.01 M electrolyte solution, maximum electropositive and electronegative zeta potentials, ζ = +4.3 mV and ζ = –13.8 mV occurred at pH 2 and pH 11 respectively for hematite-*P. putida* interactions. In the other conditions, the zeta potential reduces with increasing concentration to 0.05 M, and increases back in a solution concentration of 0.1 M. The zero-point charge (PZC) is reduced from pH 4.8 in 0.01 and 0.05 M solution to pH 3.2 in 0.1 M electrolyte solution in hematite-*P. putida* solutions. Without bacteria, the PZC is reduced from pH 4.0 for low ionic strengths to pH 3 at 0.1 M.

The effect of the hematite's grain size on the surface's electrical potential has been investigated by zeta potential behaviour of hematite (grain sizes of <10 μm, 50–250 μm, and 500–1,000 μm) with and without *P. putida* at 0.01 M NaCl (Fig. 5). Similar zeta potential values of electropositive charges with the point of zero charge, PZC of around pH 3.2 and 4.2 are obtained for both 50–250 μm and 500–1,000 μm hematite grain size respectively. However, the zeta potential of the fine hematite (<10 μm) is far more positive (ζ = +22.5 at pH 3) and its PZC (ζ = 0) is at pH 7.3.

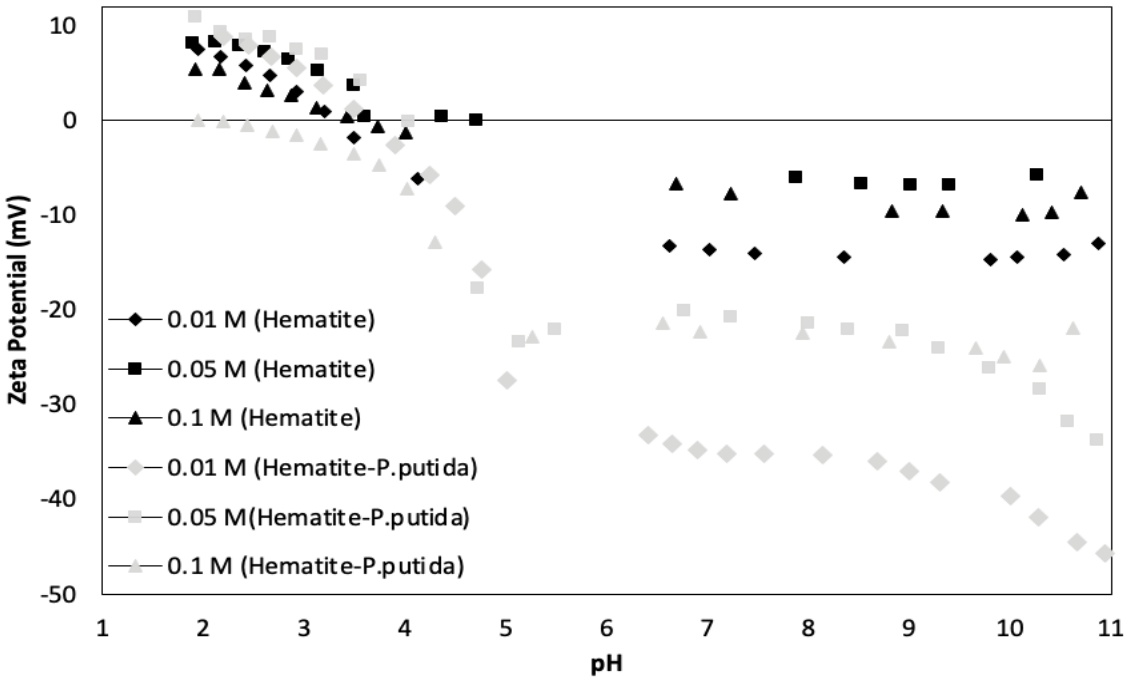

Fig. 3. Zeta potential of hematite grains (50–250 μm) with and without *Pseudomonas putida* suspension in various electrolyte concentrations.

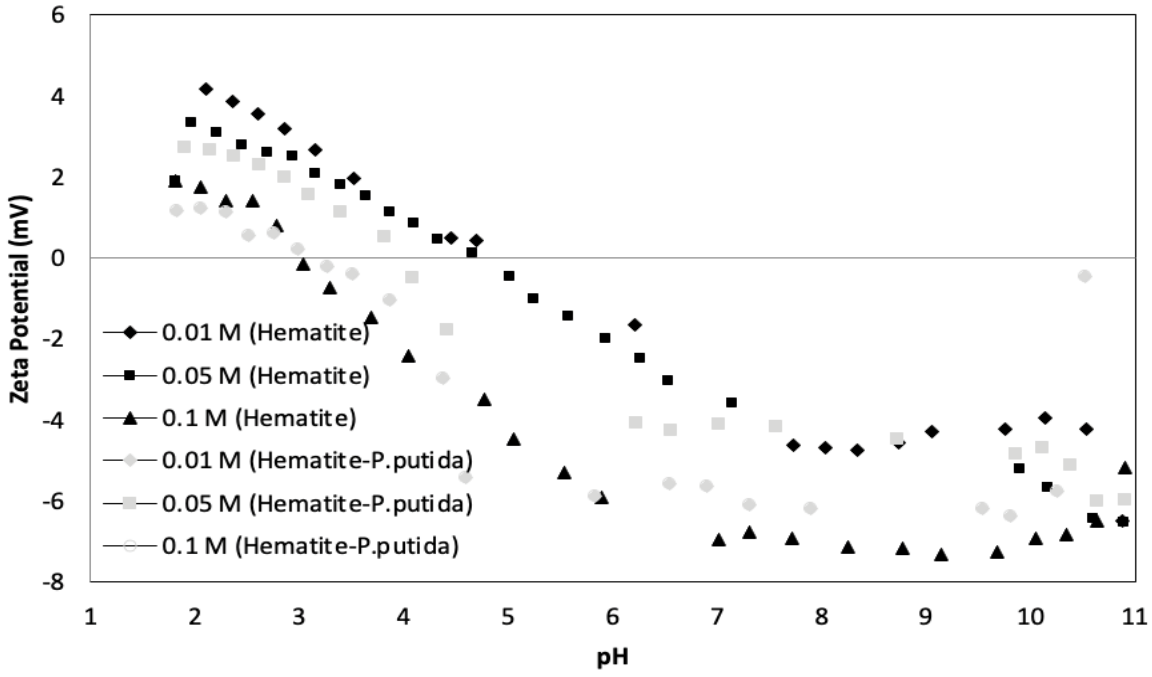

Fig. 4. Zeta potential of hematite grains (500–1,000 μm) with and without *Pseudomonas putida* suspension in various electrolyte concentrations.

The smaller particle size shows very high negative zeta potentials compared to the coarser particles for hematite with *P. putida* solutions. However, an obvious gap between the zeta potential curves can be observed between hematite alone and hematite-*P. putida* interactions for the fine particles and the smaller grains, while the coarser grain size produced similar charge distributions for both conditions, which are more electropositive at all pH values.

The effect of ionic strength on the zeta potential of quartz grains with a size between 50 and 250 μm without

bacteria is shown in Fig. 6. The results reveal that the quartz surface is negatively charged for all pH values above its point of zero charge at pH 2.8. As the electrolyte concentration increases, the salt will affect the zeta potential values, which become less negatively charged due to its lower electronegativity (the tendency to attract electrons towards the particle surface). At higher electrolyte concentrations, the EDL will collapse and the zeta potential approaches zero. At this point, PZC is determined which depends only on the pH of the solution.

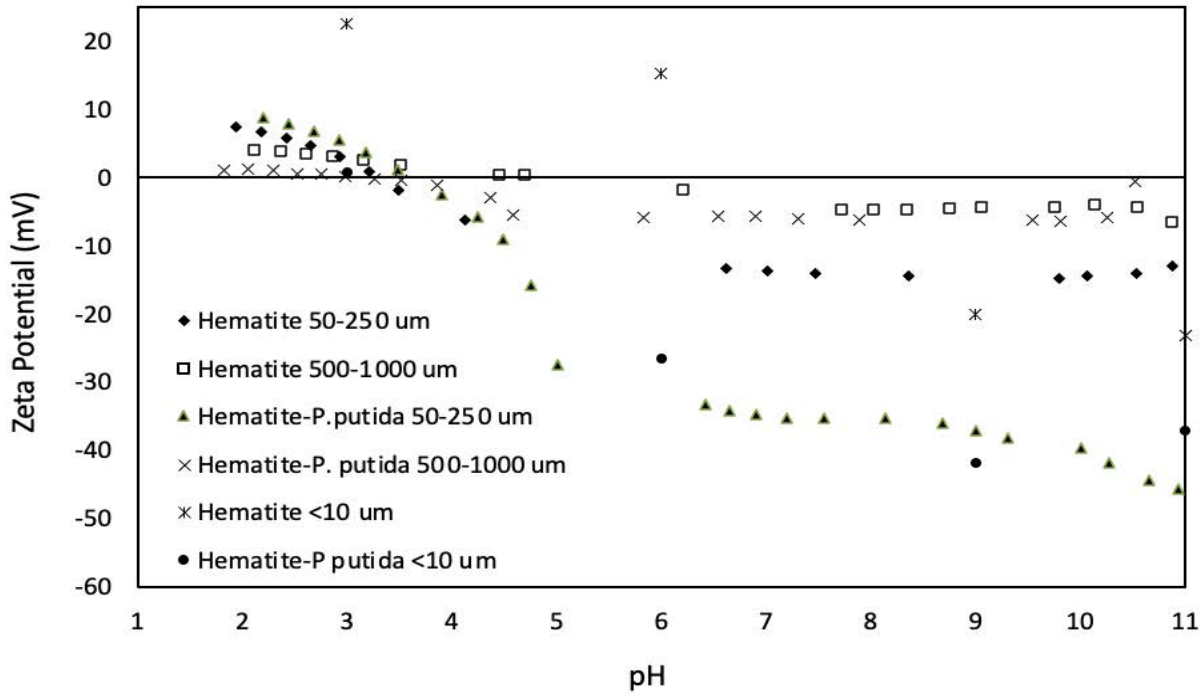

Fig. 5. Effect of the hematite grain size (<10 μm, 50–250 μm, and 500–1,000 μm) on the electrical potential of the surface, with and without *Pseudomonas putida*.

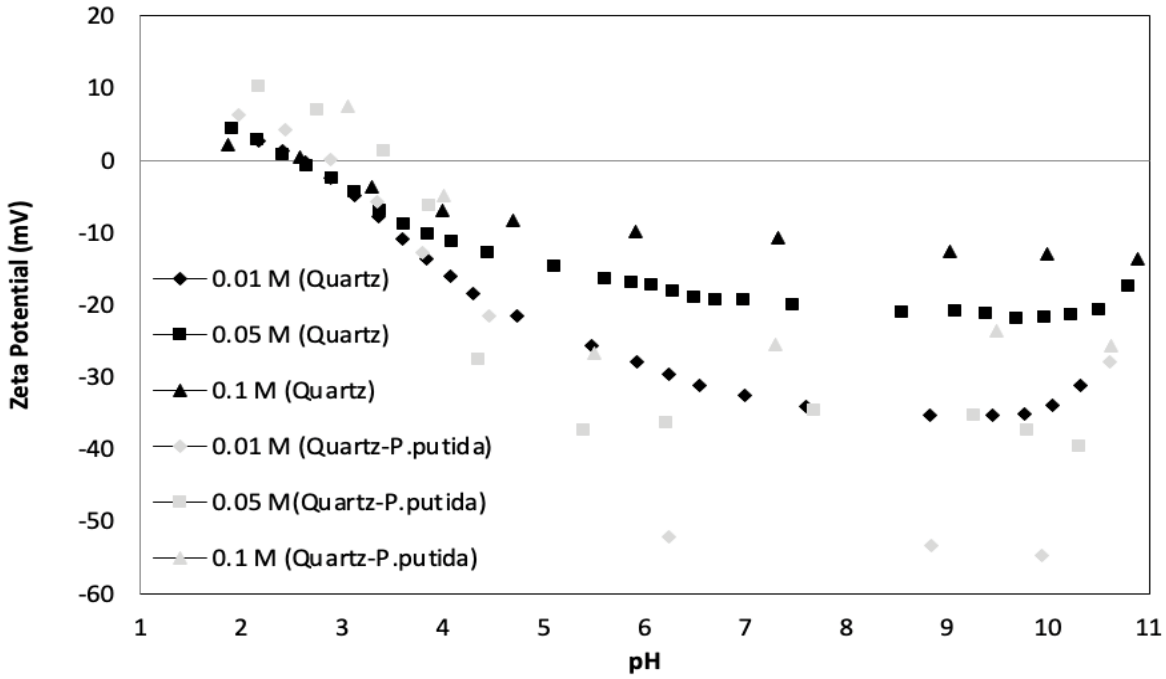

Fig. 6. Zeta potential of quartz grains (50–250 μm) with and without *Pseudomonas putida* suspension in various electrolyte concentrations.

The zeta potential of quartz grain size 50 to 250 μm with *P. putida* at different ionic strengths indicate that the interaction surfaces are more negatively charged, to –55 mV, above pH 4 producing a repulsive interaction between quartz and *P. putida*. It can be observed that the zeta potential values are higher at lowest ionic strength over all the pH range including the electropositive and electronegative charge regions. The point of zero charge for a solution with concentration 0.01 M is pH 2.8 while 0.05 and 0.1 M, it is around pH 3.5.

Fig. 7 presents the zeta potential behaviour of quartz particles with grain size of 500–1,000 μm. At 0.01 M ionic strength, the zeta potential is more positive in the acidic region and changes to very negative in the neutral and alkaline regions. Different behaviour was observed in other concentrations, where the zeta potential changes slightly from positive to negative throughout the pH range but a clear gap is seen between the two concentrations especially in the alkaline region.

It can be observed that by addition of the bacteria to the surface of the quartz, in the acidic region, the zeta potentials (between 0 and +5 mV) are close to each other at all ionic strengths. The zeta potential becomes more negative with increasing pH above the PZC. At higher pH regions there is no difference in zeta potential between 0.01 and 0.05 M, but in 0.1 M, the zeta potential is more positive than both lower ionic strengths.

The results of this section indicate that the zeta potential is obviously influenced by the presence of bacteria, electrolyte concentration and pH regions. The change in zeta potential values, without a change of PZC indicates that the electrical double layer is compressed with increasing electrolyte concentration. The ions in solution are not being adsorbed to the surface but merely building up and compressing the electrical double layer [34,35]. According to Bunt et al. [36], when protein is bound to hydrophobic ligands in aqueous solutions, the binding between them may increase when the surface tension of water is increased by the addition of salts, thereby increasing the size of the zeta potential. At low ionic strength, and in absence of polyvalent ions, intermediate adhesion may occur due to moderate charge potential, whilst at higher ionic strength better adhesion would be due to an increase in potential.

3.2. Surface hydrophobicity effect on bacterial adhesion

Epifluorescence images of *P. putida* attachment to hematite and quartz coupons are shown in Fig. 8. The images were taken at 10, 30 and 60 min for hematite and at 10, 20 and 45 min for quartz. A rolling motion was observed when the bacteria approached the mineral surface. The hydrophobicity property of the mineral coupons was measured before and after adhesion. Researchers have found that hydrophobicity of surfaces influences microbial attachment [37–40]. In this study *P. putida* show preference for surface wetting characteristics. *P. putida* adhered in greater numbers to hematite coupons while much less attachment is found on the quartz coupons (Fig. 8). At pH 5–6, at all ionic strengths, the bacteria adhered more on the hematite surface (up to 30 cells per captured area (50 μm^2)). As the hydrophobicity of hematite (contact angle, θ = 46.2) is higher than quartz (contact angle, θ = 28.4), the bacteria, which is less hydrophobicity (contact angle, θ = 38.5) with a high negative charge on its membrane surface, is more attracted to the more hydrophobic surface (hematite) as reported by Hwang et al. [41].

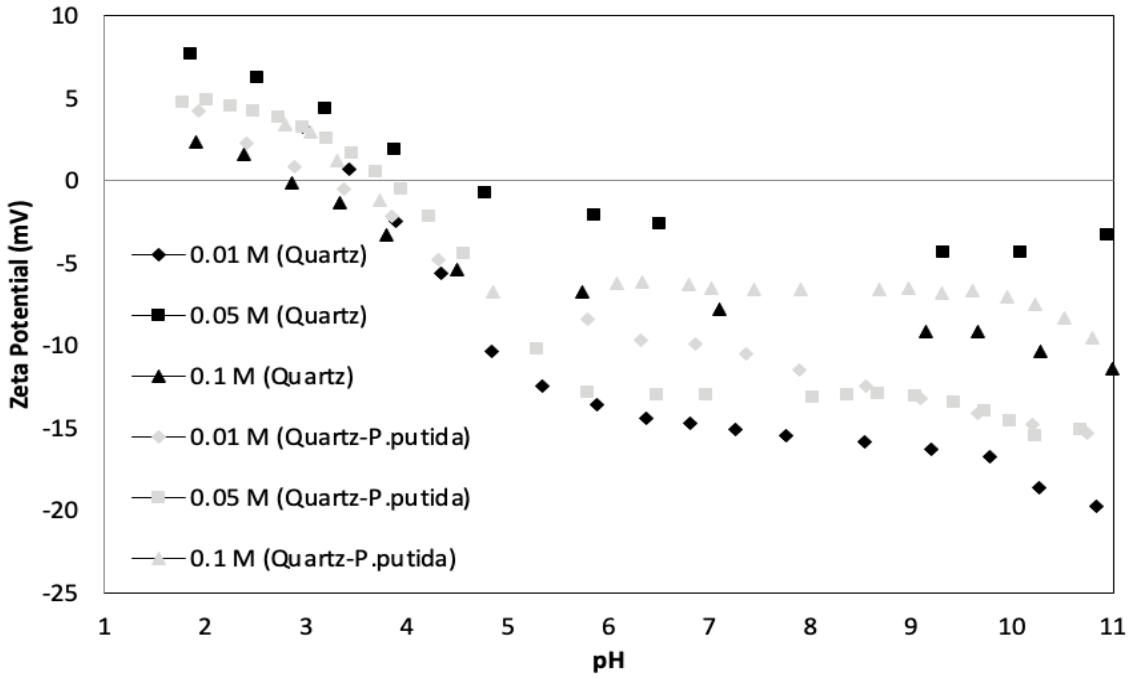

Fig. 7. Zeta potential of quartz grains (500–1,000 μm) with and without *Pseudomonas putida* suspension in various electrolyte concentrations.

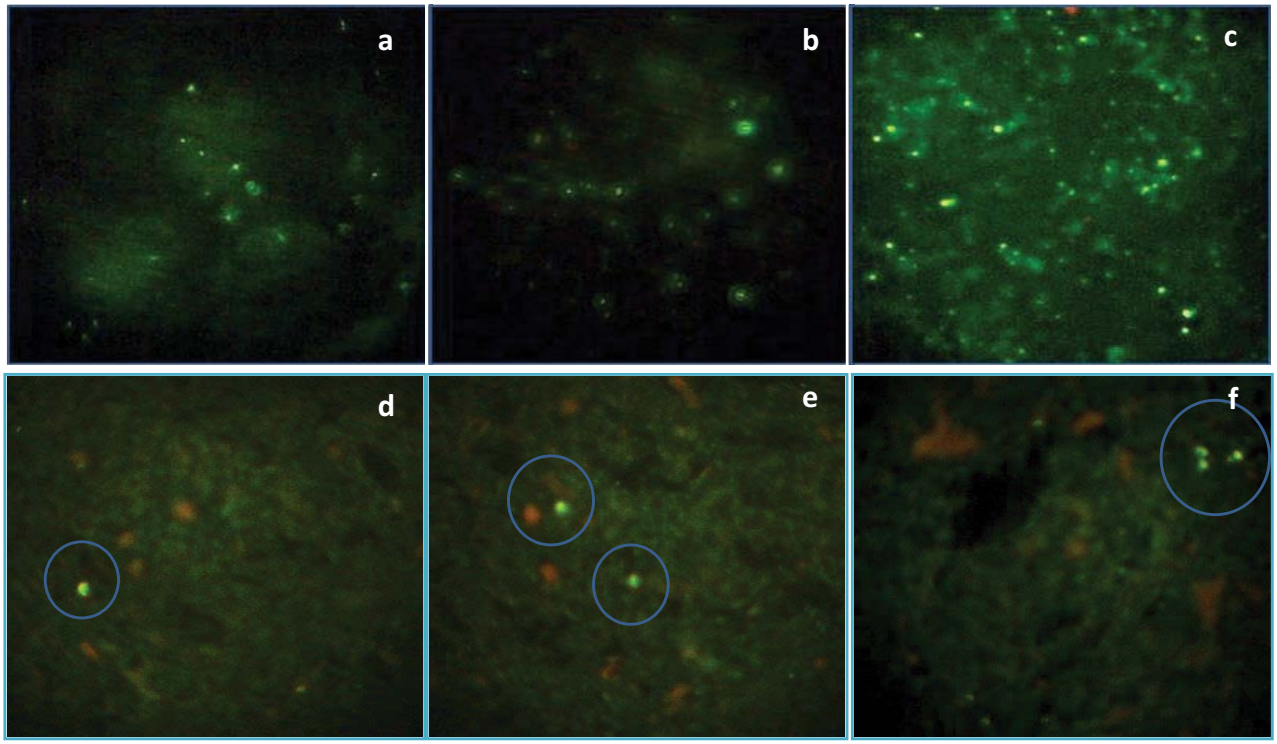

Fig. 8. *Pseudomonas putida* attachment to hematite and quartz coupons in 0.1 M NaCl at pH 5–6 in 50 μm² (a) hematite, 10 min, (b) hematite, 30 min, (c) hematite, 60 min, (d) quartz, 10 min, (e) quartz 20 min, and (f) quartz, 45 min.

3.3. Effect of pH and ionic strength on bacterial adhesion to the hematite and quartz minerals

According to the reports by many researchers, bacterial adhesion behaviour and surface hydrophobicity is influenced by electrolyte ionic concentration and pH of the solution [42–45]. The hydrophobicity was found to be significantly lower at higher pH, and low ionic strength while there is greater cell surface hydrophobicity at lower pH values and higher ionic strength [46]. The wettability properties of different kinds of mineral surface also give different effects.

Flow cell experiments were performed to study the impacts of the pH and electrolyte ionic concentration on the bacterial adhesion on the mineral surfaces. The influence of the pH values of the solutions on bacterial adhesion is shown in Fig. 9. The attachments of *P. putida* to mineral substrates are clearly dependent on pH, which, with ionic strength, significantly influences the cell surface hydrophobicity. At an ionic strength of 0.1 M, an increase in pH affects bacterial attachment on both mineral surfaces. At this concentration, the attachments of bacteria at pH 5–6 is higher than in the other pH conditions as reported by Kosmulski et al. [47]. The attachment of bacteria onto hematite at pH 2–3 and pH 10–11 are much lower than attachment at pH 5–6.

For quartz, there was a small effect of pH different where the highest attachment is at pH 5–6 (number of bacterial attached, n = 3) and only one bacterium was attached at pH 10–11 (Fig. 9). Extreme acidic and basic solutions may produce a higher gap in charge distribution on the bacteria surface, which is influenced by different concentrations of hydrogen and hydroxyl groups in the solution [48]. However, the bacterial attachment on hematite is still greater than quartz at both pH 2–3 and pH 10–11. The maximum attachment occurs at pH 5–6 and an ionic strength of 0.1 M NaCl and the minimum attachment was at pH 10–11 and ionic strength of 0.01 M.

Previous reports found that bacterial attachment is higher in solutions whose pH is near to the surface's point of zero charge, PZC [33,49,50]. For hematite, the results obtained follow this trend where the PZC is around pH 4–5. However, for quartz, the PZC from the zeta potential measurement was near pH 2 but results show lower attachment at pH 2–3 than at pH 5–6. It has been reported that, at higher ionic strengths, charge effects on the bacterial cell surface may be more pronounced resulting in greater adhesion. Greater ionic strength may increase adherence by suppressing the thickness of the diffuse double layer [36], and increased the zeta potential value. At a very high salt concentration, the EDL will collapse, and the zeta potential becomes zero, resulting in no repulsion and allowing more bacterial attachment on the surface. The effect of ionic strength on the attachment of *P. putida* to the mineral coupons is presented in Fig. 10.

The greatest adhesion was found at pH 5–6 and an ionic strength 0.1 M on hematite coupons. With increasing ionic strength from 0.01 to 0.1 M. there were slight increases in attachment of *P. putida* to hematite, but these were more marked for quartz. The extended Derjaguin–Landau–Verwey–Overbeek (XDLVO) theory of colloid stability has been used as an explanation for this increase

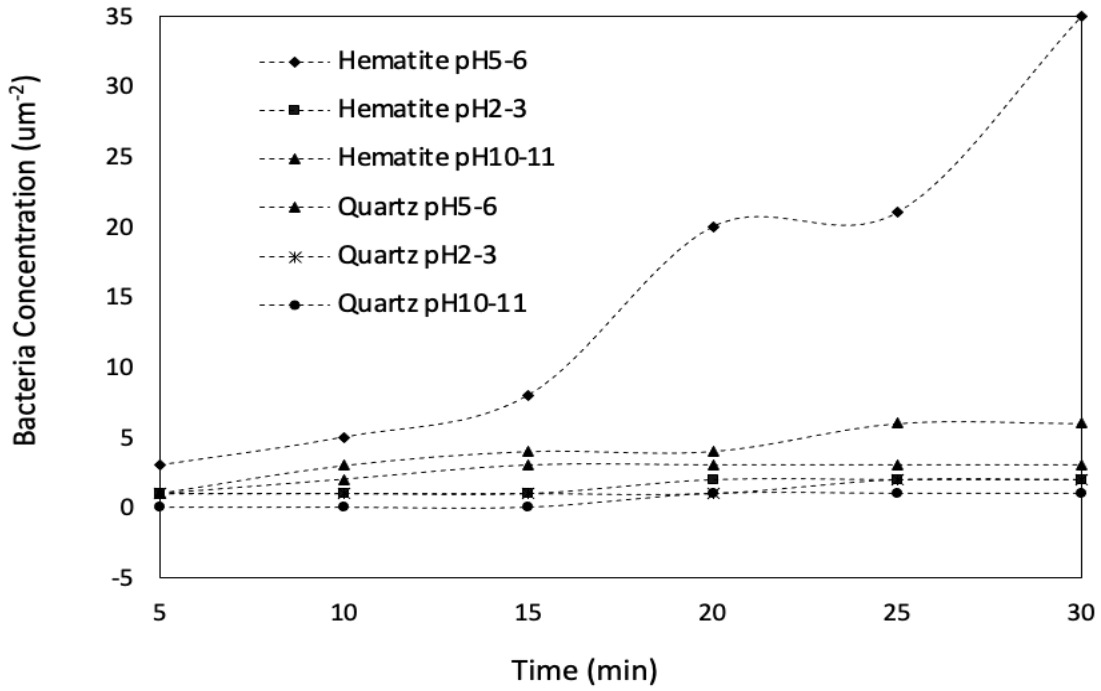

Fig. 9. Number of *Pseudomonas putida* attached to hematite and quartz at various pH values at an ionic strength of 0.1 M NaCl as a function time. The experiments were performed at flow rate of 1 mL/min under laminar flow (Re = 0.16), for 60 min, with bacterial suspension of 1×10^8 cells/mL of *Pseudomonas putida*, at 25°C and atmospheric pressure, in a parallel flow chamber.

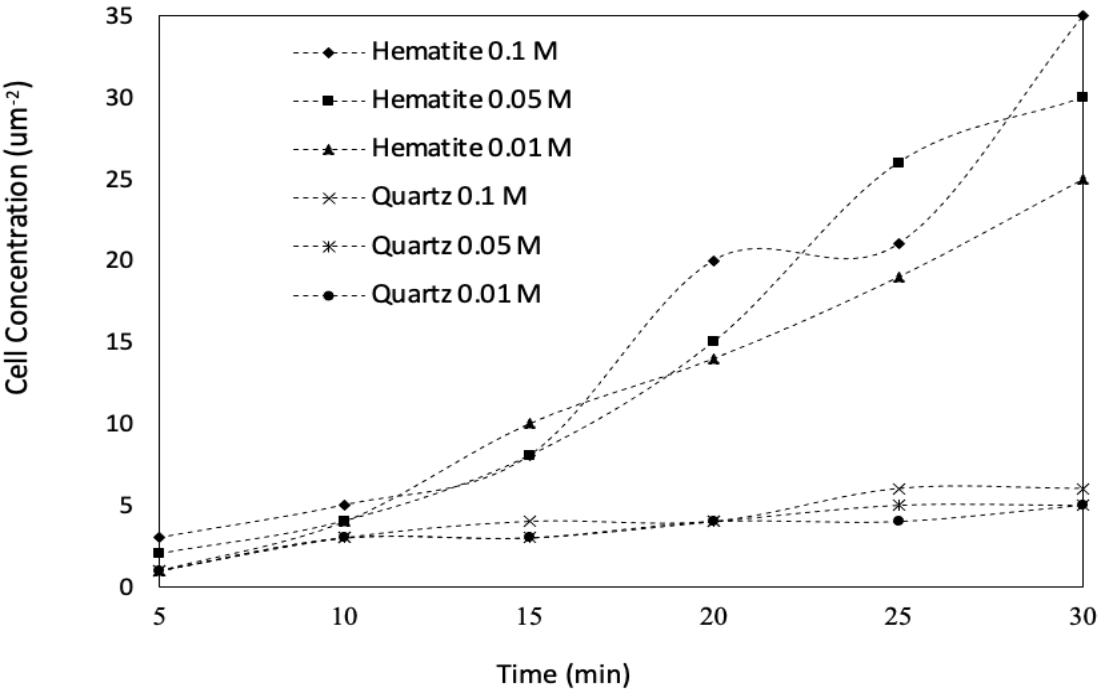

Fig. 10. Number of *Pseudomonas putida* attached to hematite and quartz in various electrolyte concentrations at pH 5–6. The experiments were performed at flow rate of 1 mL/min under laminar flow (Re = 0.16), for 60 min, with bacterial suspension of 1×10^8 cells/mL of *Pseudomonas putida*, at 25°C and atmospheric pressure, in a parallel flow chamber.

in attachment with ionic strength. The effect of increased ionic strength is suggested to be due to the suppression of the solvation barrier and negligible electrostatic interactions (repulsive) [51].

Other properties that also influence cell attachment are surface stability, and hardness. Surface stability is described by the surface potential (zeta potential, z), while the hardness can be described with reference to Mohr's scale.

3.4. XDLVO interaction energies

The XDLVO theory describes attachment in terms of the sum of repulsive acid-base and electrostatic interaction energies, and attractive van der Waals interaction energies at pH 5–6 and 0.1 M as shown in Figs. 11 and 12 for hematite and quartz, respectively. *P. putida*, hematite and quartz are all negatively charged and therefore, the bacteria-mineral substrate charge interaction is theoretically repulsive [52]. The acid-base interaction for the mineral-bacteria interaction is highly repulsive but this energy operates only at close distances of about 0.3 Å. Even though hematite has a lower van der Waals attraction energy there is attractive total interaction energy between *P. putida* and hematite due to low acid-base and electrostatic repulsion energies (Fig. 11) with a deeper primary minimum indicating the irreversible adhesion. The interaction energy between *P. putida* and quartz was dissimilar. Quartz has a very high acid-base repulsion energy compared to electrostatic repulsion energy (Fig. 12). This leads to more repulsive total interaction energy between quartz and *P. putida* and even with a higher van der Waals attractive energy was compared to hematite; the total repulsion energy for quartz is higher than hematite. Therefore, higher attachment is predicted on hematite. This is demonstrated experimentally by the number of *P. putida* attached to hematite from the current flow-cell experiment.

The total XDLVO interaction energy as a function of separation distance of hematite and quartz interactions with *P. putida* at three different concentrations is shown in Fig. 13. According to the XDLVO theory an increase in ionic strength leads to a shielding of repulsive potentials and a favouring of attractive interactions. Thus, increasing ionic strength should lead to increased attachment for both minerals. Although the two minerals do exhibit the same trends with increasing ionic strength, the attachment of *P. putida* to hematite is much higher than the attachment to quartz for the same ionic strength.

4. Conclusions

In this investigation, we have surveyed the effects of some physio-chemical characteristics of bacterial-mineral interactions such as ionic strength and acidity of the solution. The outcomes revealed that the zeta potential is obviously influenced by the presence of bacteria, electrolyte concentration, and pH regions. At higher ionic strengths, charge effects on the bacterial cell surface increase adherence by suppressing the thickness of the diffuse double layer. Furthermore, a systematic bacterial attachment experiment using a parallel-plate flow cell has been designed to examine the influence of pH and ionic strength on bacteria to mineral surface attachment under constant flow conditions. Extreme acidic and basic conditions resulted in less attachment at lower electrolyte concentrations. Bacterial adhesion was greatest at pH 5–6 in 0.1 M ionic strength. The results were compared with the predictions from the XDLVO calculations. From this study, it can be concluded that electrolyte concentration and pH play a major role in the attachment of *P. putida* to mineral surfaces. An increase in electrolyte concentration results in an increase in attachment. Attachment on to hematite coupon was more than that of quartz at any given condition. Bacterial adhesion was also found to be dependent on pH with maximum attachment around pH 5–6. The higher attachment of *P. putida* to hematite is also influenced by hydrophobicity and surface hardness.

Interaction energy calculations using XDLVO theory correlate well with the experimental results. The major contribution to the total interaction energy (G^{TOT}), was from repulsive acid-base interaction energy (G^{AB}), which is higher for quartz compared to hematite. The interaction energy was found to become more attractive with an

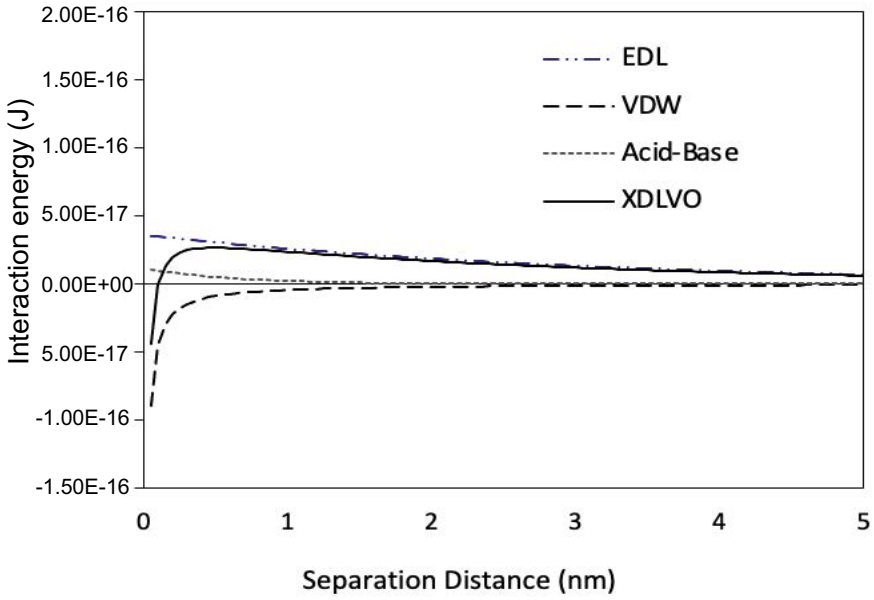

Fig. 11. XDLVO interaction energies of *Pseudomonas putida* to hematite coupon.

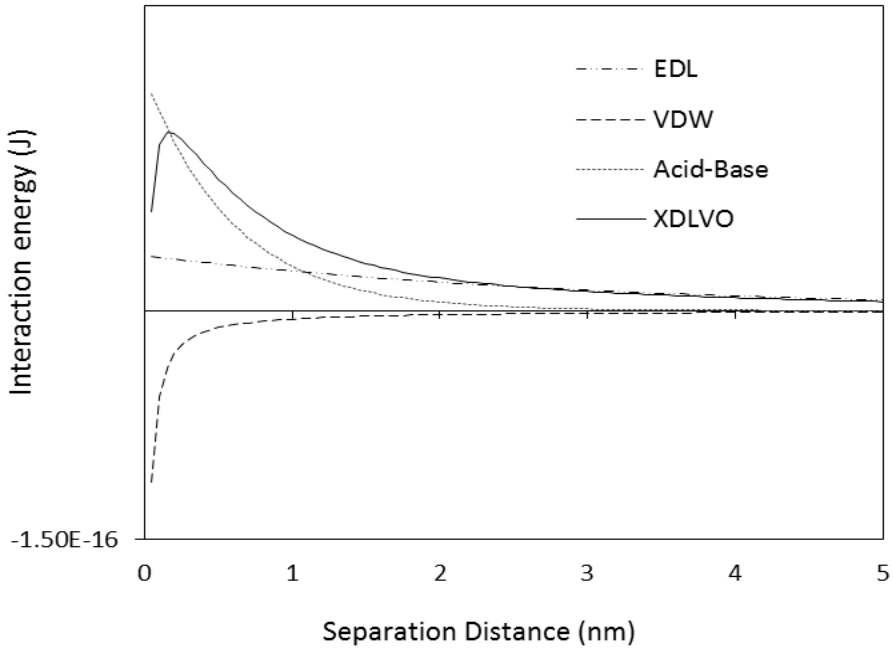

Fig. 12. XDLVO interaction energies of *Pseudomonas putida* to quartz coupon.

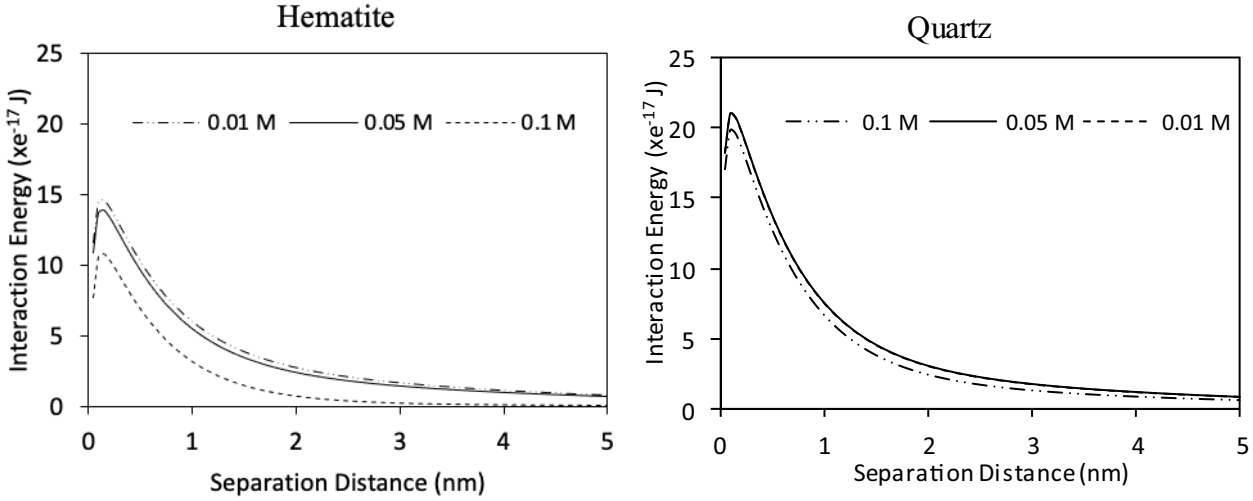

Fig. 13. XDLVO interaction energies at different ionic strength for *Pseudomonas putida* interaction to hematite and quartz minerals surfaces.

increase in electrolyte concentration thus accounting for the increase of attachment of the *P. putida* to the mineral coupon.

Declaration of competing interest

The authors declare that they have no known competing financial interests or personal relationships that could have appeared to influence the work reported in this paper.

Acknowledgement

This project was funded by University of Malaya, Faculty Research Grant, under grant No. (GPF 028A-2019) and No. (RF 006A-2018). The authors, therefore, gratefully acknowledge the financial support.

References

[1] F.G. Martins, A. Melo, S.F. Sousa, Databases for the study of biofilms: current status and potential applications, Biofouling, 37 (2021) 96–108.
[2] B.P. Singh, S. Ghosh, A. Chauhan, Development, dynamics and control of antimicrobial-resistant bacterial biofilms: a review, Environ. Chem. Lett., 19 (2021) 1983–1993.
[3] L.D. Blackman, Y. Qu, P. Cass, K.E.S. Locock, Approaches for the inhibition and elimination of microbial biofilms using macromolecular agents, Chem. Soc. Rev., 50 (2021) 1587–1616.
[4] J. Caro-Astorga, E. Frenzel, J.R. Perkins, A. Álvarez-Mena, A. de Vicente, J.A.G. Ranea, O.P. Kuipers, D. Romero, Biofilm

formation displays intrinsic offensive and defensive features of *Bacillus cereus*, npj Biofilms Microbiomes, 6 (2020), doi: 10.1038/s41522-019-0112-7.
[5] M. Jamal, W. Ahmad, S. Andleeb, F. Jalil, M. Imran, M. Asif Nawaz, T. Hussain, M. Ali, M. Rafiq, M. Atif Kamil, Bacterial biofilm and associated infections, J. Chin. Med. Assoc., 81 (2018) 7–11, doi: 10.1016/j.jcma.2017.07.012.
[6] Q. Liu, J. Wang, R. He, H. Hu, B. Wu, H. Ren, Bacterial assembly during the initial adhesion phase in wastewater treatment biofilms, Water Res., 184 (2020) 116147, doi: 10.1016/j.watres.2020.116147.
[7] K. Liu, P. He, H. Bai, J. Chen, F. Dong, S. Wang, M. He, S. Yuan, Effects of dodecyltrimethylammonium bromide surfactant on both corrosion and passivation behaviors of zinc electrodes in alkaline solution, Mater. Chem. Phys., 199 (2017) 73–78.
[8] J. Dong, Y. Wang, L. Wang, S. Wang, S. Li, Y. Ding, The performance of porous ceramsites in a biological aerated filter for organic wastewater treatment and simulation analysis, J. Water Process Eng., 34 (2020) 101134, doi: 10.1016/j.jwpe.2020.101134.
[9] R. Farber, I. Dabush-Busheri, G. Chaniel, S. Rozenfeld, E. Bormashenko, V. Multanen, R. Cahan, Biofilm grown on wood waste pretreated with cold low-pressure nitrogen plasma: utilization for toluene remediation, Int. Biodeterior. Biodegrad., 139 (2019) 62–69.
[10] A. Gran-Scheuch, E. Fuentes, D.M. Bravo, J.C. Jiménez, J.M. Pérez-Donoso, Isolation and characterization of phenanthrene degrading bacteria from diesel fuel-contaminated Antarctic soils, Front. Microbiol., 8 (2017) 1634, doi: 10.3389/fmicb.2017.01634.
[11] V. Vishwakarma, Impact of environmental biofilms: industrial components and its remediation, J. Basic Microbiol., 60 (2020) 198–206.
[12] H.F.S. Gafri, F.M. Zuki, M.K. Aroua, N.A. Hashim, Mechanism of bacterial adhesion on ultrafiltration membrane modified by natural antimicrobial polymers (chitosan) and combination with activated carbon (PAC), Rev. Chem. Eng., 35 (2019) 421–443.
[13] H.F. Gafri, F.M. Zuki, M.K. Aroua, M.M. Bello, Enhancing the anti-biofouling properties of polyethersulfone membrane using chitosan-powder activated carbon composite, J. Polym. Environ., 27 (2019) 2156–2166.
[14] T. Roger Garrett, M. Bhakoo, Z. Zhang, Bacterial adhesion and biofilms on surfaces, Prog. Nat. Sci., 18 (2008) 1049–1056.
[15] M.E. Cortés, J.C. Bonilla, R.D. Sinisterra, Biofilm formation, control and novel strategies for eradication, Sci. Against Microbiol. Pathog. Commun. Curr. Res. Technol. Adv., 2 (2011) 896–905.
[16] D.J. Davidson, D. Spratt, A.D. Liddle, Implant materials and prosthetic joint infection: the battle with the biofilm, EFORT Open Rev., 4 (2019) 633–639.
[17] C.E. Foster, M. Kok, A.R. Flores, C.G. Minard, R.A. Luna, L.B. Lamberth, S.L. Kaplan, K.G. Hulten, Adhesin genes and biofilm formation among pediatric *Staphylococcus aureus* isolates from implant-associated infections, PLoS One, 15 (2020) e0235115, doi: 10.1371/journal.pone.0235115.
[18] K. Hori, S. Matsumoto, Bacterial adhesion: from mechanism to control, Biochem. Eng. J., 48 (2010) 424–434.
[19] A. Blazyte, A.B. Alayande, T.-T. Nguyen, R.S. Adha, J. Jang, M.M. Aung, I.S. Kim, Effect of size fractioned alginate-based transparent exopolymer particles on initial bacterial adhesion of forward osmosis membrane support layer, J. Ind. Eng. Chem., 94 (2021) 408–418.
[20] J. Chen, Y. Shi, D. Cheng, Y. Jin, W. Hutchins, J. Liu, Survey of pathogenic bacteria of biofilms in a metropolitan drinking water distribution system, FEMS Microbiol. Lett., 366 (2019) fnz225, doi: 10.1093/femsle/fnz225.
[21] X. Wu, J. Pan, M. Li, Y. Li, M. Bartlam, Y. Wang, Selective enrichment of bacterial pathogens by microplastic biofilm, Water Res., 165 (2019) 114979, doi: 10.1016/j.watres.2019.114979.
[22] M. Fernández, M. Porcel, J. de la Torre, M.A. Molina-Henares, A. Daddaoua, M.A. Llamas, A. Roca, V. Carriel, I. Garzón, J.L. Ramos, M. Alaminos, E. Duque, Analysis of the pathogenic potential of nosocomial *Pseudomonas putida* strains, Front. Microbiol., 6 (2015) 871, doi: 10.3389/fmicb.2015.00871.
[23] H. Liu, S. Li, X. Xie, Q. Shi, *Pseudomonas putida* actively forms biofilms to protect the population under antibiotic stress, Environ. Pollut., 270 (2021) 116261, doi: 10.1016/j.envpol.2020.116261.
[24] F. Mohamed Zuki, R.G.J. Edyvean, H. Pourzolfaghar, N. Kasim, Modeling of the van der Waals forces during the adhesion of capsule-shaped bacteria to flat surfaces, Biomimetics, 6 (2021) 5, doi: 10.3390/biomimetics6010005.
[25] H. Wu, D. Jiang, P. Cai, X. Rong, K. Dai, W. Liang, Q. Huang, Adsorption of *Pseudomonas putida* on soil particle size fractions: effects of solution chemistry and organic matter, J. Soils Sediments, 12 (2012) 143–149.
[26] E.V. Shein, N.V. Verkhovtseva, E.Y. Milanovsky, A.A. Romanycheva, Microbiological modification of kaolinite and montmorillonite surface: changes in physical and chemical parameters (model experiment), Biogeosystem Tech., 9 (2016) 229–234.
[27] L. Krause, D. Biesgen, A. Treder, S.A. Schweizer, E. Klumpp, C. Knief, N. Siebers, Initial microaggregate formation: association of microorganisms to montmorillonite-goethite aggregates under wetting and drying cycles, Geoderma, 351 (2019) 250–260.
[28] A. Putnis, R. Hinrichs, C.V. Putnis, U. Golla-Schindler, L.G. Collins, Hematite in porous red-clouded feldspars: evidence of large-scale crustal fluid–rock interaction, Lithos, 95 (2007) 10–18.
[29] X. Wang, B. Liu, X. Pan, G.M. Gadd, Transport and retention of biogenic selenium nanoparticles in biofilm-coated quartz sand porous media and consequence for elemental mercury immobilization, Sci. Total Environ., 692 (2019) 1116–1124.
[30] T.H. Ong, E. Chitra, S. Ramamurthy, C.C.S. Ling, S.P. Ambu, F. Davamani, Cationic chitosan-propolis nanoparticles alter the zeta potential of *S. epidermidis*, inhibit biofilm formation by modulating gene expression and exhibit synergism with antibiotics, PLoS One, 14 (2019) e0213079, doi: 10.1371/journal.pone.0213079.
[31] S. Ramezaniankeikanloo, Multiscale Investigations of the Effects of Chemical Stimuli on the Composition, Adhesion and Mechanics of *Pseudomonas putida* Cells and Biofilms, Ph.D. Thesis, Washington State University, ProQuest Dissertations Publishing, 2018.
[32] J.-Z. He, D.-J. Wang, H. Fang, Q.-L. Fu, D.-M. Zhou, Inhibited transport of graphene oxide nanoparticles in granular quartz sand coated with *Bacillus subtilis* and *Pseudomonas putida* biofilms, Chemosphere, 169 (2017) 1–8, doi: 10.1016/j.chemosphere.2016.11.040.
[33] M. Farahat, T. Hirajima, K. Sasaki, K. Doi, Adhesion of *Escherichia coli* onto quartz, hematite and corundum: extended DLVO theory and flotation behavior, Colloids Surf., B, 74 (2009) 140–149.
[34] A.R. Shashikala, A.M. Raichur, Role of interfacial phenomena in determining adsorption of *Bacillus polymyxa* onto hematite and quartz, Colloids Surf., B, 24 (2002) 11–20.
[35] M.Z. Fathiah, R.G. Edyvean, The role of ionic strength and mineral size to zeta potential for the adhesion of *P. putida* to mineral surfaces, World Acad. Sci. Eng. Technol., Int. J. Biotechnol. Bioeng., 9 (2015) 805–810.
[36] C.R. Bunt, D.S. Jones, I.G. Tucker, The effects of pH, ionic strength and polyvalent ions on the cell surface hydrophobicity of *Escherichia coli* evaluated by the BATH and HIC methods, Int. J. Pharm., 113 (1995) 257–261.
[37] R.M. Goulter, I.R. Gentle, G.A. Dykes, Issues in determining factors influencing bacterial attachment: a review using the attachment of *Escherichia coli* to abiotic surfaces as an example, Lett. Appl. Microbiol., 49 (2009) 1–7, doi: 10.1111/j.1472-765X.2009.02591.x.
[38] A. Krasowska, K. Sigler, How microorganisms use hydrophobicity and what does this mean for human needs?, Front. Cell. Infect. Microbiol., 4 (2014) 112, doi: 10.3389/fcimb.2014.00112.
[39] C. Desrousseaux, V. Sautou, S. Descamps, O. Traoré, Modification of the surfaces of medical devices to prevent

microbial adhesion and biofilm formation, J. Hosp. Infect., 85 (2013) 87–93.
[40] Y. Liu, S.-F. Yang, Y. Li, H. Xu, L. Qin, J.-H. Tay, The influence of cell and substratum surface hydrophobicities on microbial attachment, J. Biotechnol., 110 (2004) 251–256.
[41] G. Hwang, C.-H. Lee, I.-S. Ahn, B.J. Mhin, Analysis of the adhesion of *Pseudomonas putida* NCIB 9816-4 to a silica gel as a model soil using extended DLVO theory, J. Hazard. Mater., 179 (2010) 983–988.
[42] D. Yongabi, S. Jooken, S. Givanoudi, M. Khorshid, O. Deschaume, C. Bartic, P. Losada-Pérez, M. Wübbenhorst, P. Wagner, Ionic strength controls long-term cell-surface interactions – a QCM-D study of *S. cerevisiae* adhesion, retention and detachment, J. Colloid Interface Sci., 585 (2021) 583–595.
[43] G. Hurwitz, G.R. Guillen, E.M.V. Hoek, Probing polyamide membrane surface charge, zeta potential, wettability, and hydrophilicity with contact angle measurements, J. Membr. Sci., 349 (2010) 349–357.
[44] G. Chen, S.L. Walker, Role of solution chemistry and ion valence on the adhesion kinetics of groundwater and marine bacteria, Langmuir, 23 (2007) 7162–7169.
[45] Y. Liu, Q. Zhao, Influence of surface energy of modified surfaces on bacterial adhesion, Biophys. Chem., 117 (2005) 39–45.
[46] M. Katsikogianni, Y.F. Missirlis, Concise review of mechanisms of bacterial adhesion to biomaterials and of techniques used in estimating bacteria-material interactions, Eur. Cell Mater, 8 (2004) 37–57.
[47] M. Kosmulski, E. Maczka, E. Jartych, J.B. Rosenholm, Synthesis and characterization of goethite and goethite–hematite composite: experimental study and literature survey, Adv. Colloid Interface Sci., 103 (2003) 57–76.
[48] A.T. Poortinga, R. Bos, W. Norde, H.J. Busscher, Electric double layer interactions in bacterial adhesion to surfaces, Surf. Sci. Rep., 47 (2002) 1–32.
[49] P.K. Sharma, K. Hanumantha Rao, Adhesion of *Paenibacillus polymyxa* on chalcopyrite and pyrite: surface thermodynamics and extended DLVO theory, Colloids Surf., B, 29 (2003) 21–38.
[50] L.M.S. de Mesquita, F.F. Lins, M.L. Torem, Interaction of a hydrophobic bacterium strain in a hematite-quartz flotation system, Int. J. Miner. Process., 71 (2003) 31–44.
[51] Y.-L. Ong, A. Razatos, G. Georgiou, M.M. Sharma, Adhesion forces between *E. coli* bacteria and biomaterial surfaces, Langmuir, 15 (1999) 2719–2725.
[52] C.J. van Oss, Hydrophobicity of biosurfaces — origin, quantitative determination and interaction energies, Colloids Surf., B, 5 (1995) 91–110.